ISSN: 0067-2904

Synthesis, Characterization, Molecular Docking, and *in Vitro* Screening of New Metal Complexes Derived from Acyclovir Schiff Base with Ciprofloxacin Ligand

Sahbaa Ali Ahmed*, Sariya Waleed Zedan
Department of Chemistry, College of Sciences, University of Mosul, Mousal, Iraq

Received: 25/5/2022 Accepted: 27/1/2023 Published: 30/12/2023

Abstract

In this work, combining acyclovir with ciprofloxacin (CCP), a new Schiff base and its metal complexes with iron (III), manganese (II), copper (II), zinc (II), and calcium (II) ions are synthesized and structurally characterized by XRD, SEM, ^{1}H NMR, ^{13}C NMR, FT-IR, and UV-Visible spectral techniques. Furthermore, molecular docking studies were carried out, and the complexes were tested to resolve any potential hang-ups in opposition to the Herpes virus and DFT calculation studies. In addition, the metal complexes and ligand were screened against antibacterial strains of one gram-positive bacteria (*Staphylococcus aureus*) and three gram-negative bacteria (*Escherichia coli*, *Pseudomonas aeruginosa*, and *Klebsiella pneumonia*), and it was established that these complexes demonstrate dissimilar bustles of inhibition on the enlargement of the bacteria.

Keywords: Acyclovir, Ciprofloxacin, Schiff base Complexes, Antibacterial, Herpes Virus.

تحضير، تشخيص، الالتحام الجزيئي والفحص المختبري للمعقدات الفلزية الجديدة المشتقة من قاعدة شيف الأسيكلوفير مع ليكند سيبروفلوكساسين

صهباء علي أحمد*، سارية وليد زيدان
قسم الكيمياء ، كلية العلوم ، جامعة الموصل ، العراق

الخلاصة

في هذا العمل، يتم تصنيع ودمج الأسيكلوفير مع سيبروفلوكساسين (CCP)، وقاعدة شيف الجديدة ومعقداتها المعدنية مع أيونات الحديد (III)، المنغنيز (II)، النحاس (II)، الزنك (II) والكالسيوم (II) وشخصت بواسطة تقنيات XRD، SEM، ^{1}H NMR، ^{13}C NMR و FT–IR والتقنيات الطيفية للأشعة فوق البنفسجية المرئية. علاوة على ذلك، تم إجراء دراسات الالتحام الجزيئي وتم اختبار المعقدات لحل اي حالات تعليق محتملة تتعارض مع دراسات حساب فيروس الهربس ودراسات حساب DFT. بالاضافة الى ذلك، تم فحص المعقدات المعدنية و الليكند ضد السلالات المضادة للبكتيريا لبكتيريا واحدة موجبة الكرام (*Staphylococcus aureus*) و ثلاث بكتيريا سالبة الكرام (*Escherichia coli*، *Pseudomonas aeruginosa* و *Klebsiella pneumonia*)، و قد ثبت أن هذه المعقدات تظهرغير متشابهة تثبيط على تضخم البكتيريا.

* Email: sahbaa-ali@uomosul.edu.iq

1. Introduction

Ciprofloxacin [also known as 1-cyclopro-pyl-6-fluoro-1,4-dihydro-4-oxo-7-(1-piperazinil)-3-quinolone carboxylic acid] is a fluoroquinolone that was developed in 1987 [1]. It is a famous antiseptic medication with a broad spectrum of activity that can be used to treat various infections [2,3]. Quinolones are a class of synthetic antibacterial medicines that have been in clinical use for more than thirty years, with ciprofloxacin being one of the most extensively used [4,5]. Ciprofloxacin belongs to the quinolone family of antibiotics. It is thought to be extremely effective, particularly in situations of infection by perceptive microorganisms in the breathing apparatus and urinary tract [6]. Quinolone, resting on the additional furnish, belongs to a class of antibiotics that has been widely used to treat a variety of bacterial illnesses [7]. Cifloxacin and norfloxacin are two quinolone antibiotics effective against both gram positive and gram-negative bacteria [8]. The antagonist struggle has advanced because of changes to the antigen target. One of the most significant factors contributing to the rise of DNA genes that convert super-coiling bacteria [9] because of pump inflow is the cause of numerous antibiotic resistances. As a result, the stream of antibiotics diminishes the attention given to antibiotics at their target locations [10]. L-valine, 2-[(2-amino-1,6-dihydro-6-oxo-9*H*-purin-9-yl) methoxy] ethyl ester, and monohydrochloride are the chemical names for acyclovir. Acyclovir is which has verified antiviral bustle not in favor of herpes simplex germ kinds, one (HSV-1) and two (HSV-2) and varicella zoster virus (VZV) jointly *in vivo* and *in vitro*. Because of its affinity for the enzyme thymidine kinase, which is programmed by HSV and VZV, acyclovir has a high level of discrimination. Acyclovir is converted to acyclovir monophosphate, a nucleotide analogue, by this viral enzyme. Cellular guanylate kinase converts the monophosphate to diphosphate, which is then converted to triphosphate by a number of cellular enzymes. Acyclovir triphosphate inhibits the replication of herpes virus DNA *in vitro*. Medicine compounds are lofty, lively, and frequently used these days because of their important role in the synergistic procedure of assured medications and their beneficial biological bustle [11]. The interaction of tinny and non-tinny ions improves the feasibility and efficacy of medications [12], increasing their activity compared to the same ligand [13]. The researchers are attempting to create Schiff base coordination complexes that would act as effective inhibitors of microbial development considering these facts, as well as the importance of metal complexes in medicine.

2. Experimental

2.1. Materials and methods

Starting reagents were purchased from commercial sources, including Sigma-Aldrich Chemical Company (USA), and included ciprofloxacin hydrochloride, DMF, DMSO $FeCl_3$, $MnCl_2.4H_2O$, $CuCl_2.4H_2O$, $ZnCl_2.6H_2O$, $CaCl_2.6H_2O$, and EtOH from BHD corporation. Elemental microanalysis for carbon, hydrogen, and nitrogen were recorded on a Euro Vector (replica EA3000, single) V.3.0 rudimentary scrutinize. The metal ions satisfied were premeditated as oxides of metals. Seven HANNAC214 was used to measure the molar conductivity of the ligand and its compound in black DMSO at 10^{-3} M. The magnetic measurements on the Sherwood Scientific magnetic equilibrium were obtained using the Gouy balance technique at space heat with Hg [Co $(SCN)_4$] as the calibrant. The UV-visible was obtained from a DMSO (10^{-3} M) solution for the ligand as well as the equipped compound using a spectrophotometer (Shimadzu 160A) and quartz cells (1 cm) at wave lengths ranging from 200 to 1000 nm. An FT-IR spectrophotometer (Bruker alpha, FT-IR-ATR platinum reflective) was used to measure the spectral data in the 400-4000 cm^{-1} wavelength range. The ^{13}C NMR and ^{1}H NMR spectral data were recorded using a Varian Agilent 500 MHz spectrometer in the solvent of a DMSO-d^6, even as the chemical budge was considered to approximately peak in the black. The (TG) was performed in a lively *N* ambiance (20 mL per minute) with rapid heat (10 °C) per minute using a thermal analyzer (Perkin Elmer TG 4000). Antiseptic motion was resolved using the compact disk dispersal technique, XRD patterns were scanned using

diffractogram X from Phillips Holland, and SEM images were captured using ZEISS GmbH microscopy.

2.2. Antibacterial activity

The antibacterial activity of the ligand and metal complexes was tested *in vitro* against the bacteria *Staphylococcus aureus*, *Escherichia coli*, *Pseudomonas aeruginosa*, and *Klebsiella pneumonia* by means of the document disc plate process [12-15]. The complexes were tested at concentrations of 0.50 and 1.0 mg mL^{-1} in DMSO and proportionate to antibiotics. Ciprofloxacin and antiviral acyclovir were tested in DMSO at 250 and 500 ppm concentrations and compared with the control.

2.3. Synthesis

2.3.1. Synthesis of CCP

The new Schiff base 1-cyclopropyl-6-fluoro-4-(6-hydroxy-9-(2-hydroxyethoxy) methyl)-9*H*-purin-2-yl)imino)-7-(piperazin-1-yl)-1,4-dihydroquinoline-3-carboxylic acid (CCP) was prepared according to the literature method [13-15]. To a mixture of acyclovir (3.3 g, 15 mmol) and ciprofloxacin (4.9 g, 15 mmol) in dry ethanol (25 mL), glacial acetic acid (2-3 drops) was added (the pH solution became 4) (Scheme1). The solution was then heated to reflux for 6 hours. Following the completion of the reaction, the orange solid that precipitated was filtered with pure water, and bathed in EtOH, and dehydrated in air for an extended period of time. The yellow solid was acquired from the ethanol-acetic acid combination (Scheme 1).

2.3.2. Synthesis of metal complexes

To a hot solution of Schiff base ligand (16 mmol) in ethanol (30 mL), a hot solution of corresponding metal chlorides ($FeCl_3$, $MnCl_2.4H_2O$, $CuCl_2.4H_2O$, $ZnCl_2.6H_2O$, and $CaCl_2.6H_2O$ (8 mmol) in water (2 mL) in a molar relative amount of 1:2 (M: L), add a few drops of NaOH, was added (Scheme 1). The reaction mixture was then refluxed for 4 hours. The colored solution was condensed and cooled. Upon cooling, the precipitate was filtered and dried [13-15]. The physical properties of the obtained compounds are shown in Table 1.

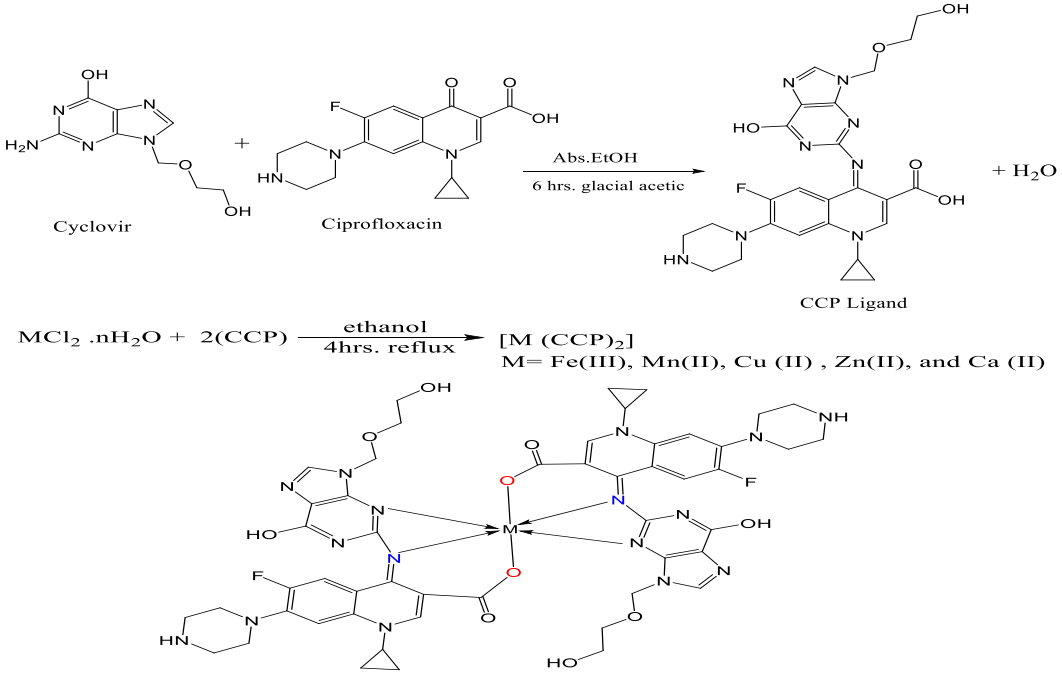

Scheme 1**:** Synthetic pathway of acyclovir, ciprofloxacin, (CCP) Schiff base ligand and its metal complexes

3. Result and discussion

3.1. General

In fundamental psychiatry, the stoichiometry and modus operandi of the gratis CCP ligand and its metal compounds were corroborated by their elemental analysis (Table 1). The metal: ligand relative amount was established to be [1:2] in every compound, which has been inferred inwards *via* approximation for the C, H, N, and Cl as well as the metal satisfies of the compounds. The fundamental psychiatry of the ligand and its complexes revealed respectable accord with the wished-for construction. The ligands and compounds have a melting point far above ground, and they were established to be atmosphere-steady. The ligand was soluble in regular, unrefined oil, and each compound was soluble in DMF and DMSO but not in CH_3OH, C_2H_5OH, or H_2O. Because of the rudimentary psychoanalytic statistics of the ligand (Table 1), it was established that the hypothetical principles were in accord with the established principles. As well as the results of elemental analyses, the formulas $[M(CCP)_2]$ (M = Mn (II), Cu (II), Zn (II), Ca (II), and $[M(CCP)_2]$ Cl (M = Fe (III)).

Table 1: Analytical and physical data of Schiff base ligand and its complexes

Compound	Color	m.p. (°C)	Yield (%)	Found (%)			
				C	H	N	**M**
CCP	Yellow bluish	210	80	55.76 (55.48)	5.05 (4.98)	20.81 (20.44)	-
Mn $(CCP)_2$	Yellow	228	66	53.15 (53.36)	4.64 (4.29)	19.83 (19.45)	**4.86 (4.62)**
[Fe $(CCP)_2$] Cl	Brown bluish	262	69	51.49 (51.70)	4.49 (4.29)	19.21 (19.50)	**4.79 (4.38)**
Cu $(CCP)_2$	Green bluish	246	68	52.74 (52.40)	4.60 (4.37)	19.68 (19.28)	**3.34 (3.10)**
Zn $(CCP)_2$	Yellowish Green	228	74	52.66 (52.70)	4.60 (4.75)	19.65 (19.70)	**5.73 (5.50)**
Ca $(CCP)_2$	Yellowish Green	222	70	53.85 (53.48)	4.70 (4.80)	20.10 (20.16)	**3.59 (3.38)**

3.2. The spectrum of ^1H NMR of the CCP ligand

The ^1H NMR spectrum of the Schiff base ligand (CCP) is shown in Figure 1. A multiple signal for the CH_2-CH_2 protons of the cyclopropane ring was observed at 1.08-1.18 ppm [16], as was a multiple signal for the NH proton between 1.93 and 198 ppm. A multiple signal from 2.93 to 2.96 ppm for CH_2-NH of the piperazine protons. The signals from 3.23 to 3.25 ppm are for CH_2-N-CH_2 protons. The range of 3.58-3.59 ppm is due to CH_2-CH_2-O protons, the signal at 3.59 ppm is for CH_2-N protons of cyclopropane, and the triplet signal at 3.6 ppm is attributed to the OH proton [17]. The signal at 3.56 ppm for the COOH proton and 5.58 ppm for N-CH_2-O protons, 7.16-7.65 ppm for aromatic protons (Ar-H), and 8.10-8.12 ppm for the HC=N amine cluster in the structure of the azomethine bond is a corroboration of the formation of the Schiff base [18,19].

3.3. The spectrum of ^{13}C NMR of the CCP ligand

The ^{13}C NMR spectrum of the ligand discloses the presence of a predictable number of signals in proportion to the dissimilar sorts of carbon atoms in the symmetric construction of the Schiff base (CCP). The ^{13}C- NMR spectrum of the Schiff base ligand (Figure 2) shows a strong NMR signal appearing at 9 ppm for the cyclopropane ring [4]. The peak is at 38 ppm for C-N [20]. Signals between 35 and 51 ppm belong to the piperazine ring. The signal is at 60 ppm for the CH_2-O aliphatic group of the ligand. Other signals are in 69-70 ppm for the ether group CH_2-O-CH_2, 106-163 ppm for aromatic rings, and 169 ppm for the azomethine bond, hence a verification of the formation of the Schiff base [19,20].

3.4. Infrared Spectra

Electronic approaches to psychoanalysis also include ligand and compound research in the 4000-400 cm^{-1} range, followed by tremor spectra [21]. In this study, infrared machinery was employed to make diagnostic compounds by comparing their spectrum to those of ligands and manufactured complexes. The Schiff base ligand and complex FT-IR band allocations are presented in Table 2. Figures 3-5 show the spectra of the ligand and various complexes. The FT-IR spectra of complexes show ligand-distinctive bands with suitable shifts due to complex formation, and the FT-IR spectra of all complexes are comparable. The presence of an azomethine group causes the free Schiff base ligand to have an absorption band of 1581 cm^{-1}.

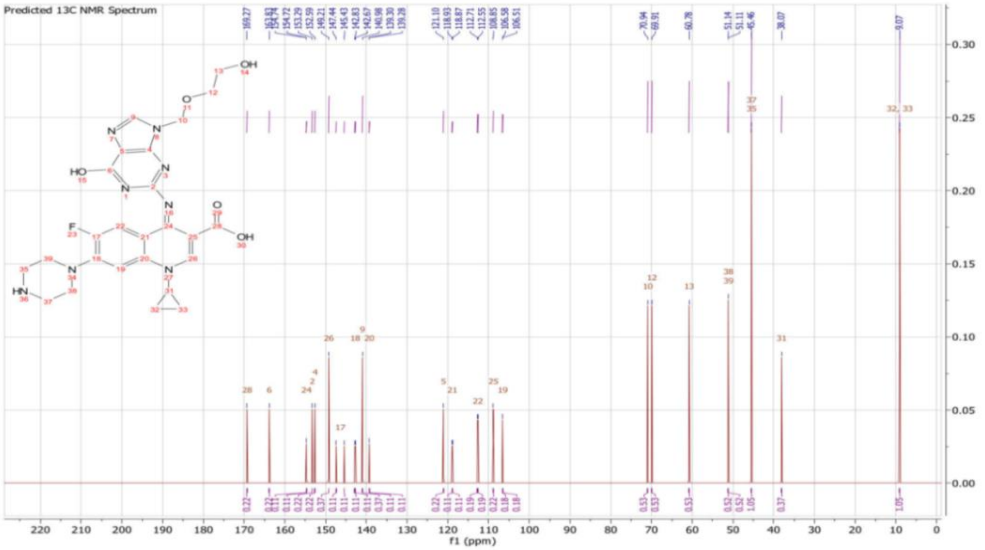

Figure 1: ^{1}H NMR spectrum of CCP ligand

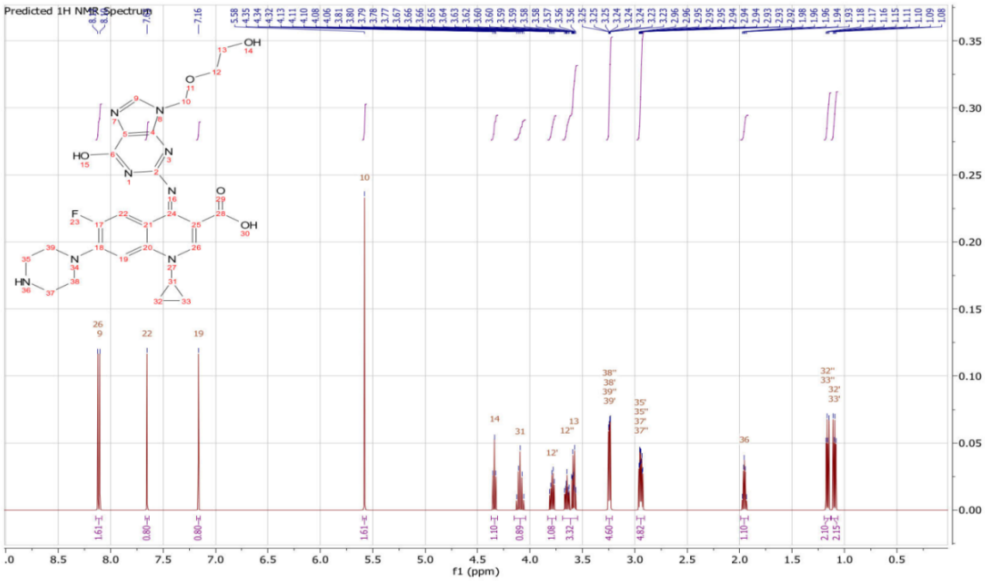

Figure 2: ^{13}C NMR scrum of CCP ligand

After complexation, these ions are moved to a lower wavenumber [22], demonstrating a physically strong double bond personality of the imine band as well as a harmonization of the azomethine nitrogen particle to the ions [6, 23]. The complexes show a strong band at 1567 cm^{-1} (C=N) stretching vibration [24]. In the spectra of metal compounds, the asymmetric stretching

vibration of COO^- posse of gratis ligand experiential at 1349-1378 cm^{-1} was moved to a lower gesticulate digit, such as 1494-1498 cm^{-1}. The asymmetric stretching vibrations of COO^- posse of free ligand observed at1379-1443 cm^{-1} was budged to inferior gesture digit in the spectrum of metal compounds 1349-1378 cm^{-1}. Symbolize carboxylic acid cluster harmonization with metal ions from end to end. The oxygen atom task of determining the desired coordination locations was further bolstered by the materialization of medium bands at 449-451 cm^{-1} and 507-508 cm^{-1}, which may exist and are attributed to the M-O and M-N stretching vibration sensations in that order [24].

Table 2: The important infrared frequencies (cm^{-1}) of the ligand and their complexes

Compound	ν(C=N)	ν(C-O)	νasmy (COO^-)	νsmy (COO^-)	ν(M-N)	ν(M-O)
CCP	1581	1158	1510	1443	-	**-**
Mn $(CCP)_2$	1562	1154	1495	1368	438	**501**
[Fe $(CCP)_2$]Cl	1567	1135	1498	1378	451	**508**
Cu $(CCP)_2$	1560	1157	1504	1373	440	**552**
Zn $(CCP)_2$	1567	1140	1494	1349	449	**507**
Ca $(CCP)_2$	1564	1156	1496	1347	448	**506**

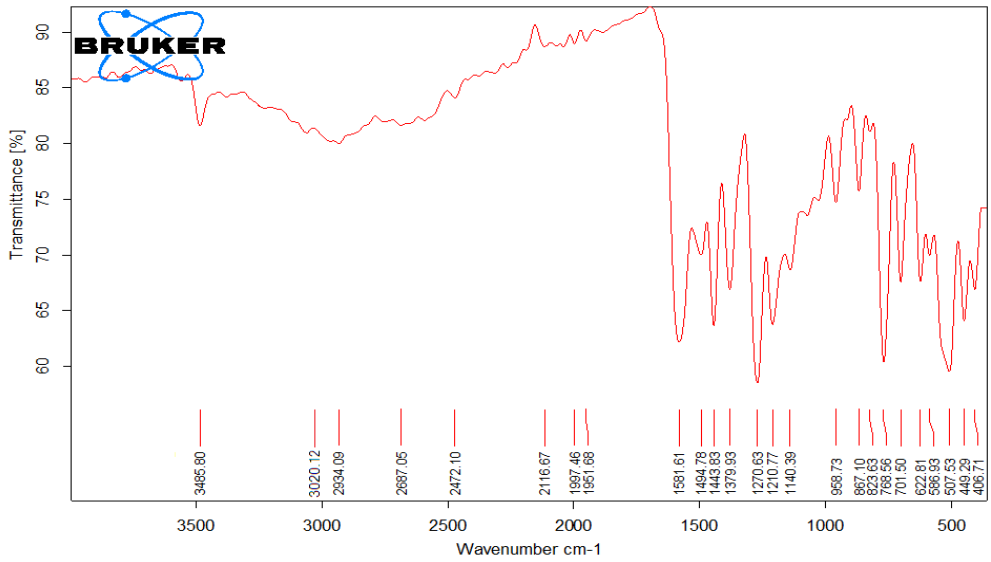

Figure 3: FT-IR spectrum of CCP ligand

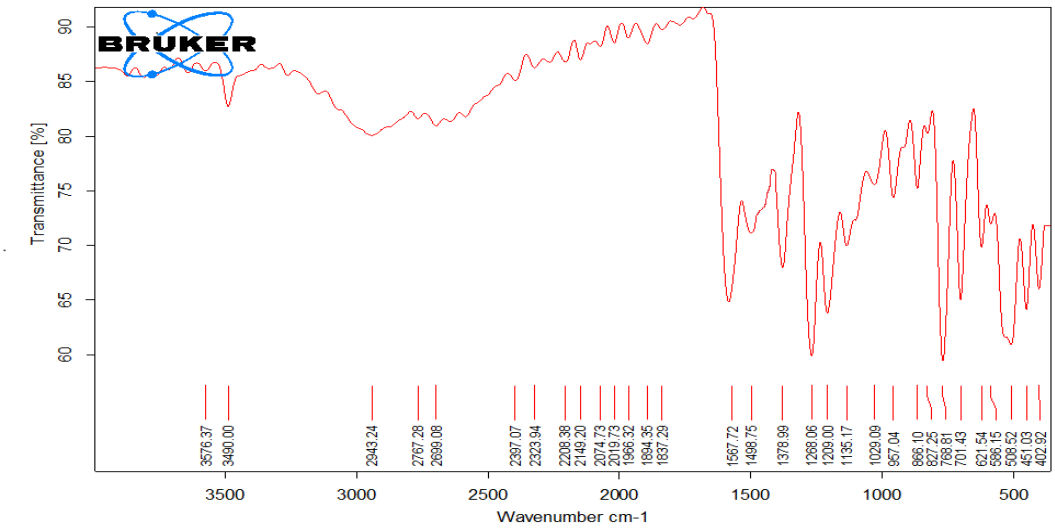

Figure 4: FT-IR spectrum of Fe (III) complex

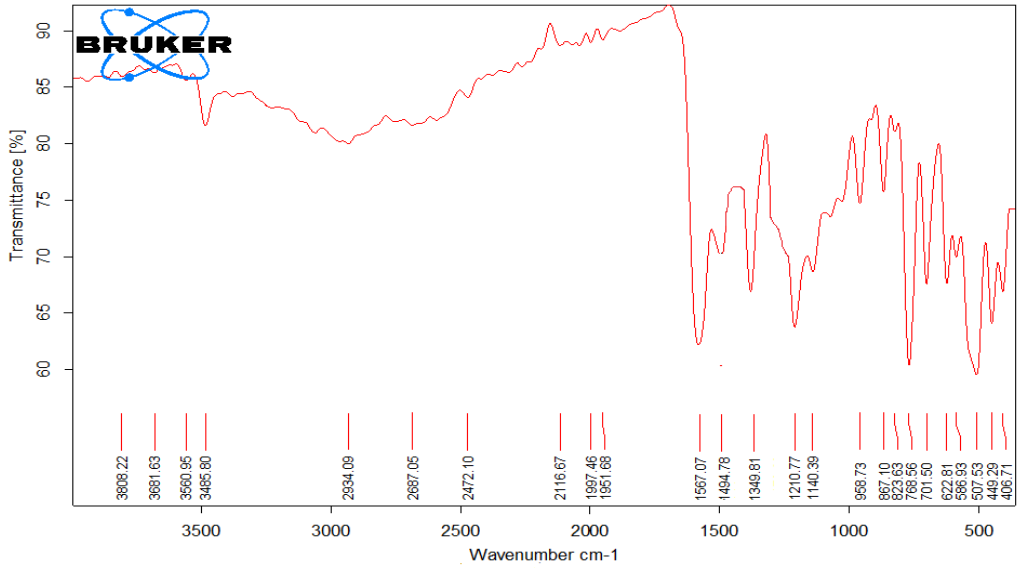

Figure 5: FT-IR spectrum of Zn (II) complex

3.5. Electronic spectra and magnetic studies

The UV-visible spectrum was measured in DMSO in the dark using a cell diameter of 1 cm and a deliberation of 10^{-3} molar at room temperature. The structure of the metal compounds was also well established by UV-visible spectra (Table 3), which demonstrates the electronic solid consideration spectra of the free Schiff base (CCP) and its metal compounds in the wavelength interval of 200 to 900 nm. The first two bands at 23202 and 30485 cm^{-1} are perhaps attributed to the n-π* and π-π* transitions [25]. The budge of the deliberation bands to higher values (bath chromic budge) and the absence of the gang at 31250 cm^{-1} in the casing of Mn (II), Fe (III), Cu (II), Zn (II), and Ca (II) composites, and the presence of original gangs in the deliberation spectra of compounds specified to their metal complex formation. The five compounds have novel bands ranging from 10490 to 27624 cm^{-1}, which could be attributed to ligand-to-metal accuse-transfer and d-d transition [26, 27]. Moreover, the Zn (II) and Ca (II) complexes have bands ranging from 24613 to 26088 cm^{-1}. Finally, the results presented here show that the magnetic moment of the Mn (II) complex is 1.79 BM and that of the Fe (III) complex is 1.83 BM, which corresponds to the stated value for the octahedral structure. The charismatic jiffy of the Cu (II) compound is 1.93 B.M., which is higher than the turn-only worth of 1.73 B.M. pro one-unpaired electron, monomeric, and well-matched, with a distorted

octahedral geometry. The Zn (II) and Ca (II) compounds were diamagnetic and had an octahedral geometry.

3.6. Molar conductivity swotes

The compounds' molar conductance (Λ_m) was measured in DMF bankrupt at 10^{-3} M attention by the side of room hotness. The soaring principles of molar conductivity of the Fe (III) compound provide 73.80 in that order, which denotes the compounds being 1:1 electrolytes with the ionic natural world as of the presence of the (Cl^-) which is situated outside of the harmonization, other than illustrated by the standards of (Λ_m) in the Mn (II), Cu (II), Zn (II), and Ca (II) complexes variety flanked by 10.6-16.00 Ω^{-1}. cm^2. mol^{-1}. This specifies that no electrolyte and no conductive genus live owing to the oxygen ions of carboxyl, which are situated inside the harmonization globe. The principles of molar conductivity of these complexes are listed in Table 3.

Table 3: The values of the electronic spectra of the ligand and its compounds, magnetic susceptibility, and molar conductance of complexes

Compound	Absorption bands(cm^{-1})	Transition	Ω^{-1}. cm^2. mol^{-1}	not compulsory geometry	µeff (BM.)
CCP	30485 23202	$\pi \rightarrow \pi^*$ $n \rightarrow \pi^*$	-	-	-
Mn $(CCP)_2$	18587 27624 30233	$^2A_1g \rightarrow {}^4T_1$ g (p) $^2A_1g \rightarrow {}^4T_1g$ (G) Center ligand	10.6	Octahedral	1.79
[Fe $(CCP)_2$] Cl	10490 19841 31210	$^2A_2g \rightarrow {}^4T_1g$ (G) $^2A_2g \rightarrow {}^4Eg$ (G) $^2A_2g \rightarrow {}^4T_1g$ (p)	73.80	Octahedral	1.83
Cu $(CCP)_2$	15650	$^2Eg \rightarrow {}^2T_2g$	12.8	Octahedral	1.93
Zn $(CCP)_2$	24613	d $\pi(Zn)^{+2} \rightarrow \pi^*(L)$	14.1	Octahedral	Dimg
Ca $(CCP)_2$	28088	d $\pi(Ca)^{+2} \rightarrow \pi^*(L)$	16.0	Octahedral	Dimg

3.7. Molecular docking study

Thymidine kinase catalyzes the phosphorylation of thymidine, preparing it for further phosphorylation and incorporation into DNA [28]. As a result, studies on the binding capacities of CCP can help create more effective HSV treatments that function as inhibitors rather than substrates of this enzyme. Docking experiments were used to analyze the ligand-receptor interactions with the herpes simplex virus type-1 thymidine kinase in this study. Auto Dock 4.2 was the program used to predict the binding affinity of chemicals [29]. Calculations for molecular docking of the enzyme crystal structures were obtained from the RCSB protein data bank (http://www.rcsb.org/pdb/) of the royal collaborator for structural bioinformatics [30]. Preparation of the chemicals and proteins [30] in order to perform molecular docking for the CCP ligand that stored them as pdbqt. The program utilized to do molecular docking was Auto Dock Vina 1.1.2 [31]. It is based on algorithms that can predict complex poses within the protein target and score them using scoring functions by configuring the grid box [32]. Figure 5 shows the docked acyclovir-ciprofloxacin (CCP) ligand inside the active site of thymidine kinase, which demonstrated 1.7841 root-mean-squared deviations. The chemicals were docked in the majority steady configuration in the active location of HSV-1 TK using energy minimization. Table 4 summarizes the docking results, and Figure 7 depicts the docking contact of complex CCP, including the active location of thymidine kinase. The oxygen of the hydroxyl group was shown to generate H-bond acceptor interactions with Ser: A100. (2.8 Å), Ala: A98132 (3.2 Å), Thr: A97, and the site was unfavorable of Alan's oxygen carbonyl group: B378, and formed C-bond acceptor interactions with Ile: B371 and Leu B440 groups of cycle

propane alkyl and double C-bond acceptor interactions with Ile: B103 group of the hexane cycle of the amino acids in the energetic position of the enzyme docking score -137.719 (kcal/mol).

Table 4: Important amino acids between thymidine kinase and CCP ligand and their contributions to binding strength

Residue	ID	Total
Thr	97	**-3.85424**
Ala	98	**-2.48774**
Ala	99	**-0.30031**
Ser	100	**-7.74995**
Ala	101	**-0.61406**
Ala	102	**-3.39683**
Ile	103	**-5.19544**
Asp	291	**-2.83478**
His	292	**-11.7905**
His	293	**-10.4678**
His	294	**-8.65541**
Arg	295	**-10.8097**
Cys	369	**-2.12277**
Ala	370	**-2.23334**
Ile	371	**-8.57909**
His	428	**-54756**
Thr	429	**-341104**
Ser	432	**-4.05123**
Asn	436	**-12.854**
Asn	437	**-12.716**
Met	439	**-1.54057**
Leu	440	**-2.92733**

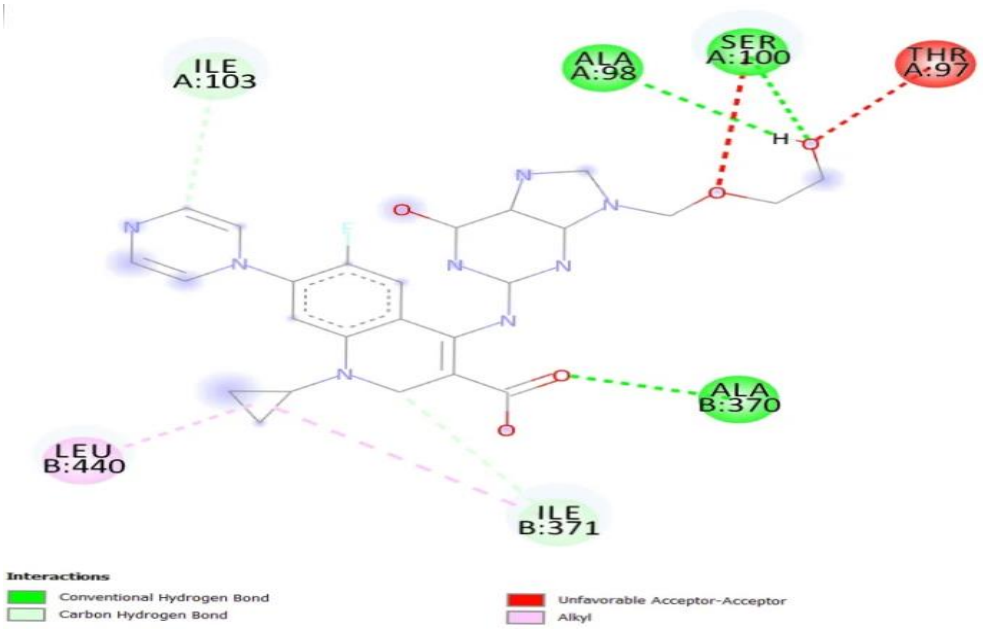

Figure 6: 2D representation of the interaction of thymidine kinase (HSV-1) with the active site of CCP Schiff base ligand

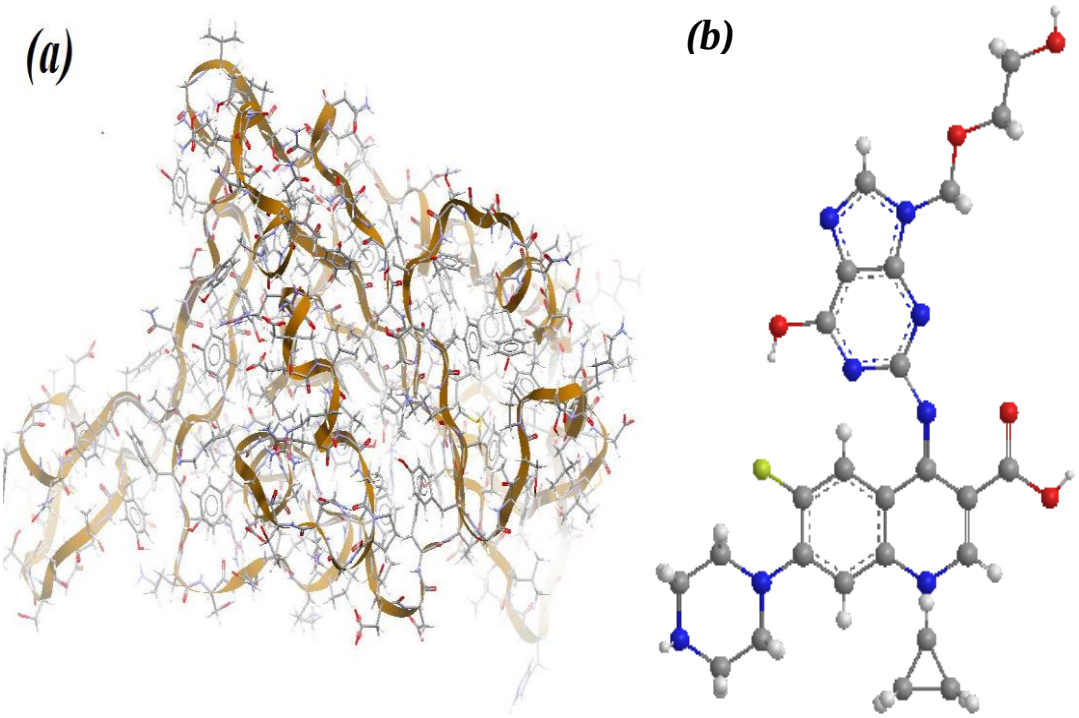

Figure 7: (a) Configuration of the protonated herpes protein for molecular and (b) Zwitter ionic CCP ligand (right) prior to docking color code: gray: C, red: O, white: H, blue: N, and yellow: F

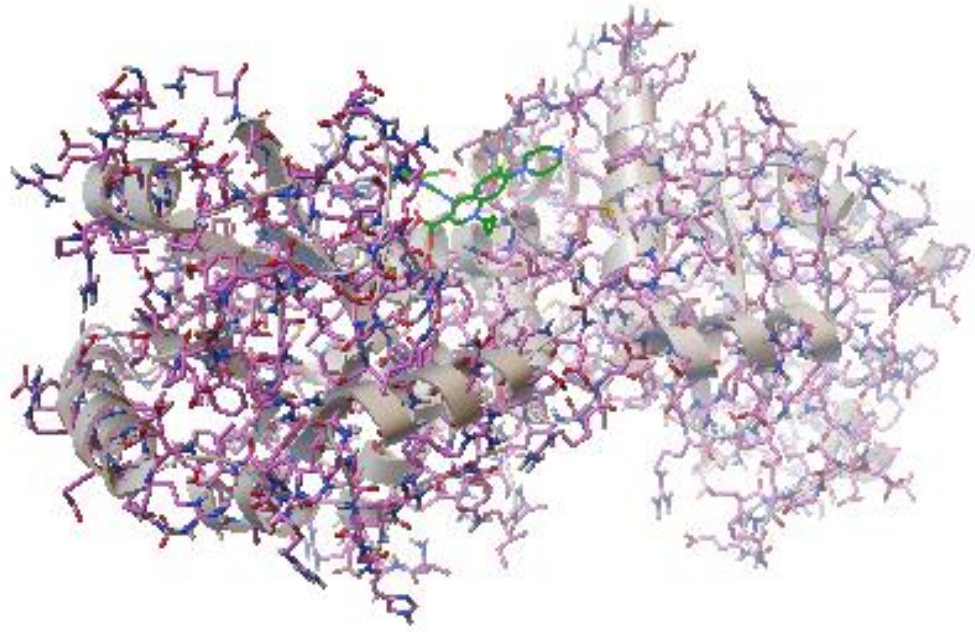

Figure 8: Initial simulation herpes protein pro molecular dynamics restfulness of ciprofloxacin-acyclovir (CCP) docked

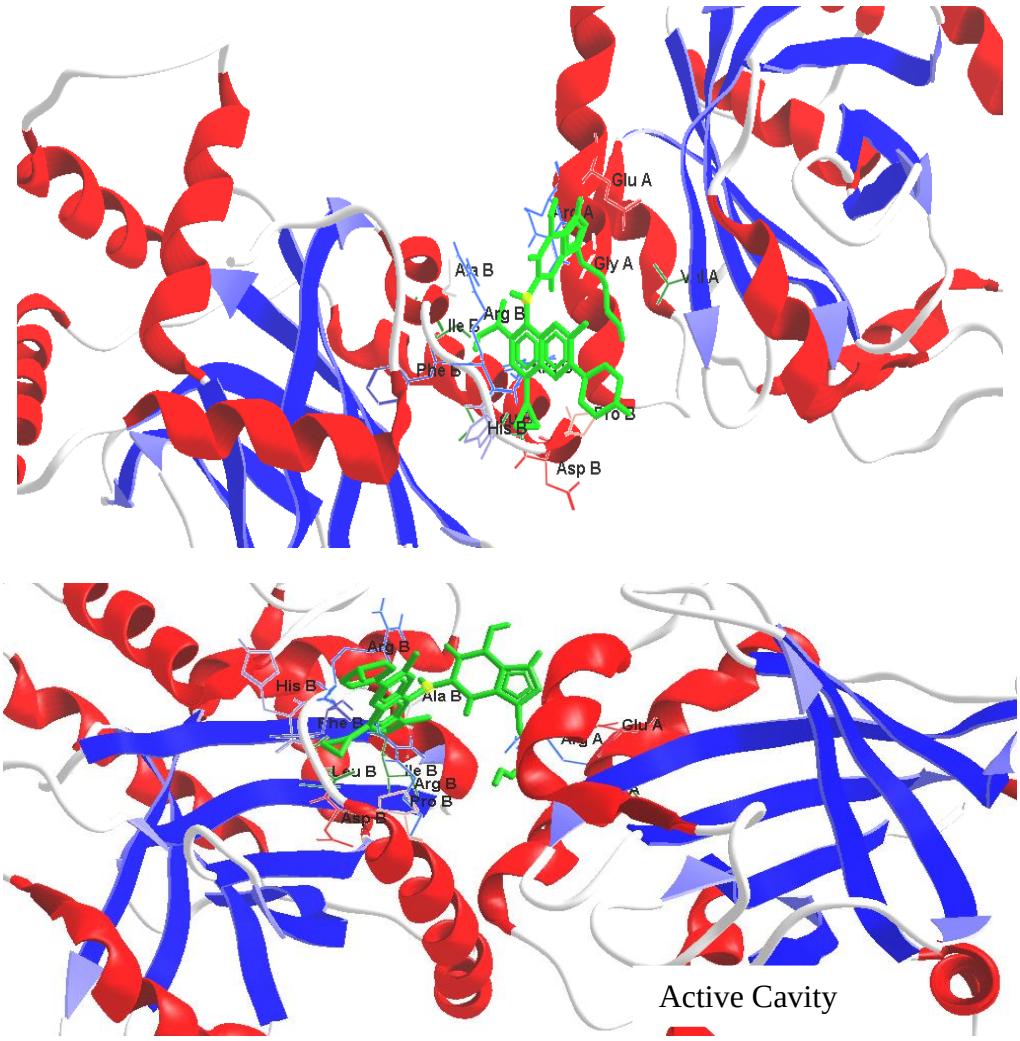

Figure 9: 3D diagrams depicting molecular docking interactions between the ligand (CCP) and protein of the herpes binding siteActive Cavity

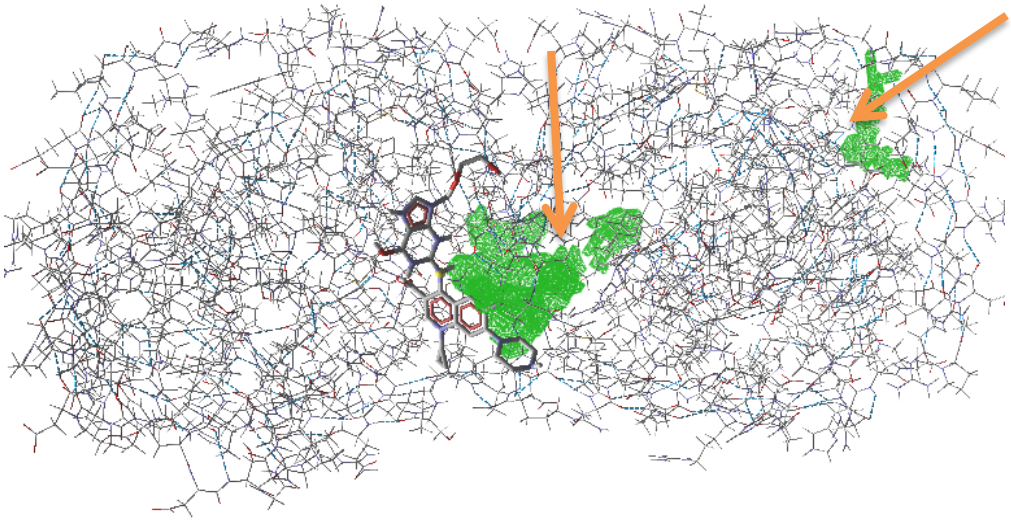

Figure 10 : Molecular binding mode of CCP ligand at the binding site of thymidine kinase (HSV-1) (green dots: active site; dashed thick green line, hydrogen bonds; unbound amino acids, steric interaction)

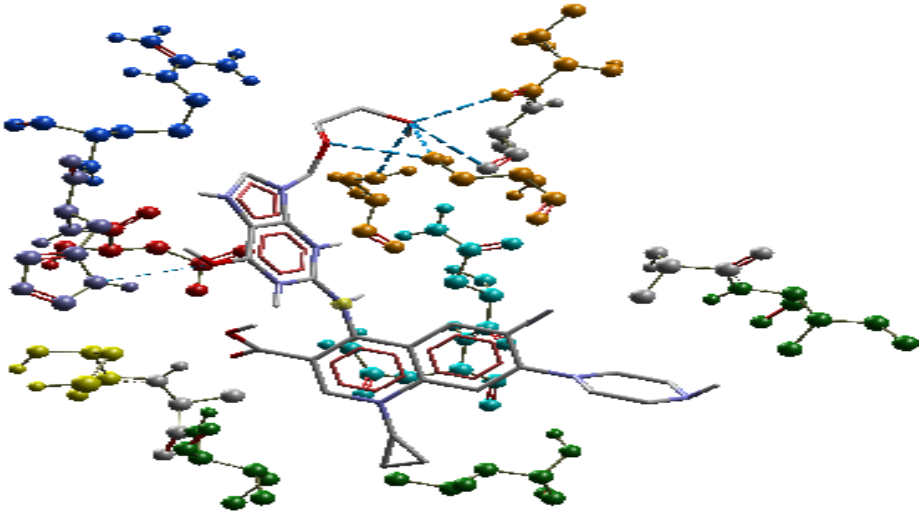

Figure 11: Molecular binding mode of CCP at the binding site of thymidine kinase (HSV-1) (hydrogen bonds and unbound amino acids)

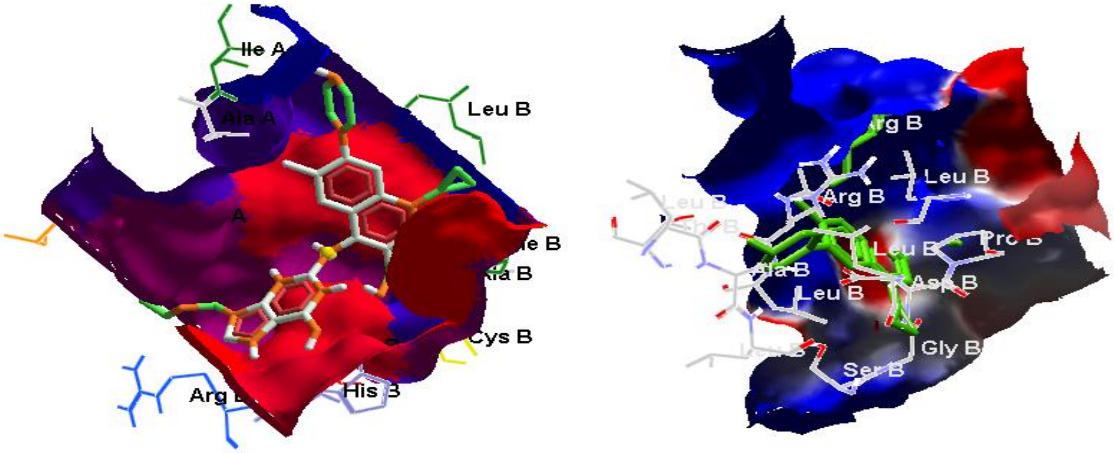

Figure 12: Hydrophilic (light blue, top) and hydrophobic (brown, bottom) districts of the ligand (CCP), and protein of herpes's binding site by molecular docking color code: gray: C, red: O, white: H, and blue: N. yellow: F.

3.8. Powder X-ray diffraction and SEM analysis.

To provide relevant crystal data, an X-ray powder diffraction approach was used to calculate precise cell parameters, crystal scheme, and cell size. The crystallographic data and powder diffraction patterns of the ligand and metal complexes are presented in Table 5. The complex's crystalline character is shown by the diffraction pattern, and the statistics verified the monoclinic crystal structure for Mn (II), Fe (III), Cu (II), Zn (II), and Ca (II) complexes. Figure 14 shows similar hexagonal crystal systems, and the ligand was tetragonal. The standards of dissimilar diffraction culmination were considered, and the atom bulk (crystallite magnitude) of compounds was designed. The small part volume can be calculated by extending the X-ray lines with the help of the following Debye Scherer method, $D = K\lambda/\beta\cos\Theta$ [33]. Anywhere, D is the particle size, K is a coefficient with a value shut towards accord; its archetypal value is equivalent to 0.89, λ is the wavelength of the X-ray, Θ is the diffraction angle acquired as of 2Θ standards in proportion to the utmost dilution climax in the XRD precedent, and β is packed breadth at semi-utmost. The standard atom bulk of the compounds, the SEM micrographs of the CCP ligand, and its Zn (II) complex are prearranged in Figure 13. There is a significant difference in the morphological construction, and the magnitude of granules is in the nanometer variety; the particle size of the ligand was 24-32 nm, even as the Zn (II) complex was 24-35 nm.

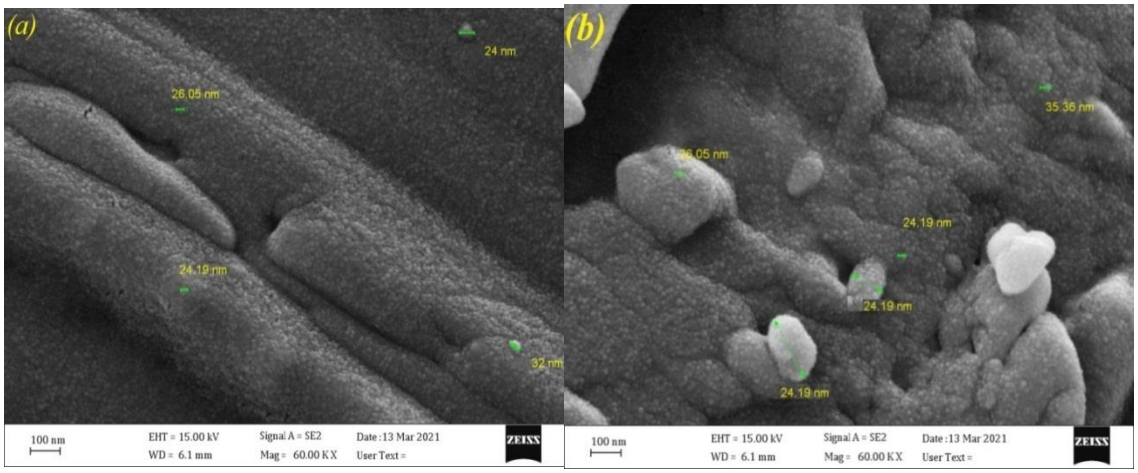

Figure 13: The SEM micrographs of ligands: (a) CCP ligand (b) Zn (II) complex

Table 5: Crystal lattice parameters of ligands and their compounds

Compound	CCP ligand	Mn (II) complex	Fe (III) complex	Cu (II) complex	Zn (II) complex	Ca (II) complex
Formula F.W(g/mol)	$C_{25}H_{27}FN_8O_5$ (538.21)	$C_{50}H_{52}F_2MnN_{16}O_{10}$ (1130.00)	$C_{50}H_{52}ClF_2FeN_{16}O_{10}$ (1165.31)	$C^{50}H_{52}CuF_2N_{16}O_{10}$ (1137.33)	$C_{50}H_{52}F_2N_{16}O_{10}Zn$ (1140.44)	$C_{50}H_{52}CaF_2N_{16}O_{10}$ (1115.14)
Wave length	1.54056	1.54056	1.54056	1.54056	1.54056	1.54056
Crystal System	Tetragonal	Monoclinic	Monoclinic	Hexagonal	Monoclinic	Hexagonal
Space group	P/mmm	P2/m	P6/mmm	P121/m1	P6/mmm	P121/m1
	Unit cell dimension					
a(Å)	12.717	1.8527	1.8643	24.7801	1.8288	24.665
b(Å)	12.717	11.429	11.785	24.7801	11.234	24.665
c(Å)	16.652	8.7017	9.2018	9.2018	8.6554	9.1244
α°	90.00	90.00	90.00	90.00	90.00	90.00
β°	90.00	97.198	9.1.226	90.00	9.2.288	90.00
γ°	90.00	90.00	90.00	120.89	90.00	120.33
Volume (Å)	2693.37	1465.68	1085.78	2678.98	1261.77	2655.82
θ range	6 - 57	11 -48	5 - 36	7 - 28	7 - 38	7- 32
Limiting indices	$0\leq h\leq 4$ $0\leq k\leq 6$ $0\leq I\leq 3$	$-6\leq h\leq 4$ $0\leq k\leq 7$ $0\leq I\leq 4$	$-10\leq h\leq 4$ $0\leq k\leq 6$ $0\leq I\leq 4$	$-1\leq h\leq 6$ $0\leq k\leq 1$ $0\leq I\leq 5$	$-6\leq h\leq 4$ $0\leq k\leq 5$ $0\leq I\leq 4$	$-1\leq h\leq 6$ $-4\leq k\leq 5$ $0\leq I\leq 7$
Particle Size (nm)	28.922	80.84	95.96	55.97	27.62	40.98
Intensity (%)	7.2-100	5.9-100	6.3-100	5.6-100	3.8-100	3.4-100
R indices	0.000015	0.000061	0.000070	0.000058	0.000052	0.000036
Density	1.0740	1.7437	1.7665	1.1355	1.034	1.01
Z	2	2	2	2	1	1

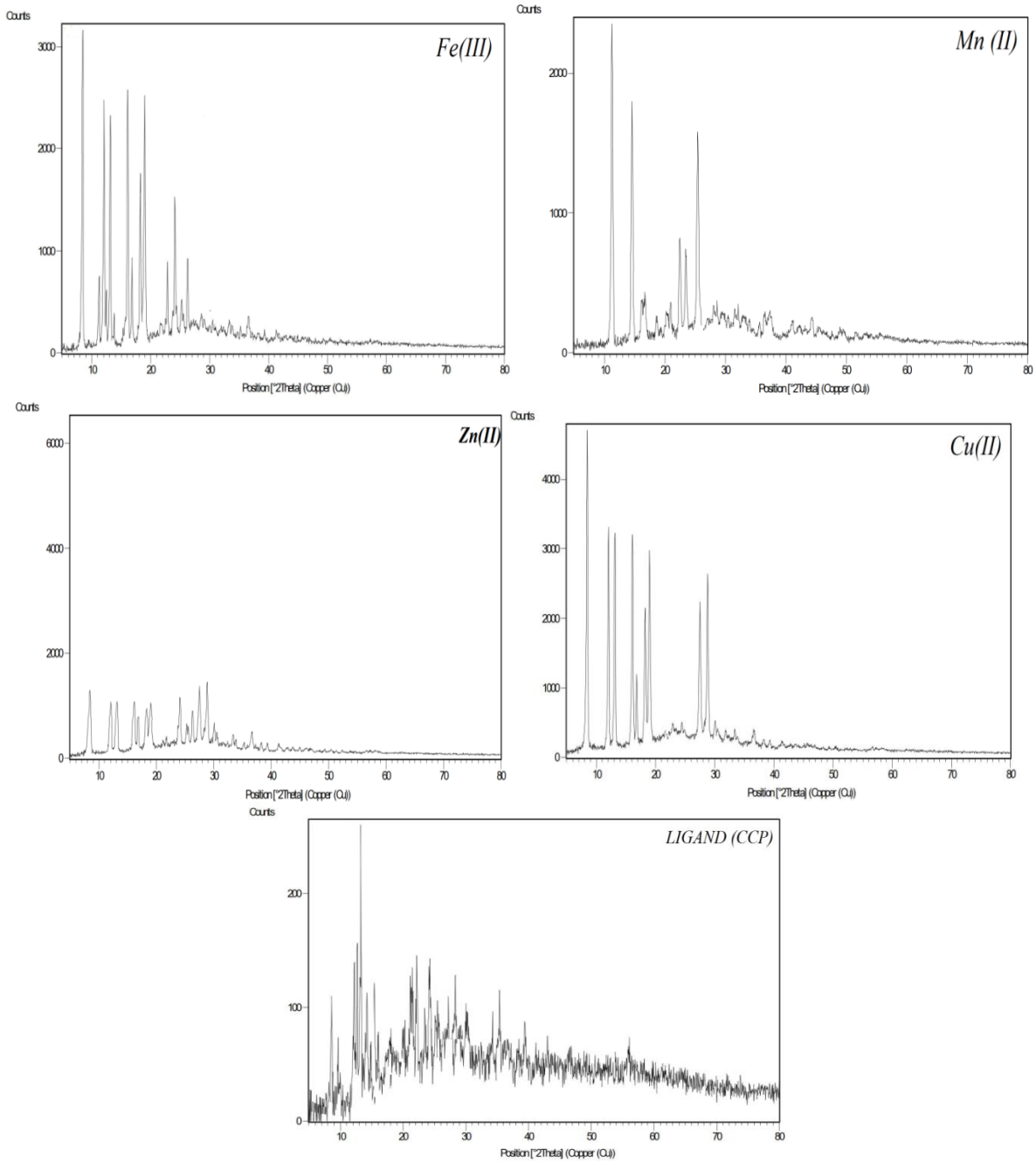

Figure 14: X-Ray diffraction patterns of the Schiff base CCP ligand and its complexes

3.9. DFT calculation studies

The boundary molecular orbitals, the uppermost engaged molecular orbital (HOMO), and the lowly untenanted molecular orbital (LUMO) are the most significant orbitals in a molecule. The boundary orbital energy gap (EHOMO – ELUMO) is a major parameter to provide details on the chemical reactivity and steadiness of the molecule and to resolve the molecular electrical properties [34,35]. A minor component, including a small force gap (DE), is associated with increased chemical reactivity (as well as near-ground chemical steadiness) and is too long tenured as a yielding molecule [35]. Figure 15 depicts the vigor gap (DE) flanked by the conspired orbitals' ability to be established *via* the DFT technique for the 3D conspires of HOMO and LUMO. The precise (HOMO – LUMO) gap energies (ΔE) of the ligand and its compounds beneath the inquisition were appraised and scheduled in Table 6. The obtained get up and go gap (DE) principles suggest the intention of regulating the chemical reactivity of the

CCP ligand, similar to its compounds: complex Fe (II) > complex Zn (II) > complex Mn (II) > complex Ca (II) > complex Cu (II) > CCP > Complex Fe (III) and complex Zn (II) are more stable than the free ligand, CCP, while other complexes (Mn, Cu, and Ca) are less stable. The chemical reactivity values: electro negativity (χ), chemical hardness (η), chemical potential (μ), electrophilicity (ω), and softness (S) of the ligand and its compounds were also designed using HOMO and LUMO energy values [$\chi = -(ELUMO + EHOMO)/2$, $\mu = -\chi = (ELUMO + EHOMO)/2$, $\eta = (ELUMO - EHOMO)/2$, $S = 1/2\eta$, $\omega = \mu 2/2\eta$, $\sigma = 1/\eta$] [36-38], and are included in Table 7. The softness (S) and electrophilicity (ω) values of the Fe (III) complex (II) are inferior to those of the ligand, and at the bottom of that, the stability of this compound is superior to that of the free ligand, in dissimilarity to the additional complexes (see Figure 16).

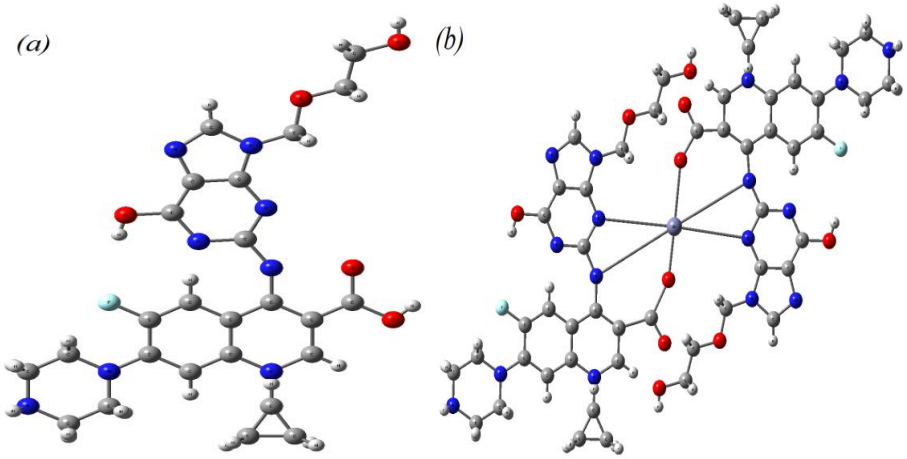

Figure 15: Optimized geometry; (a) The ligand (b) The Fe (II) complex.

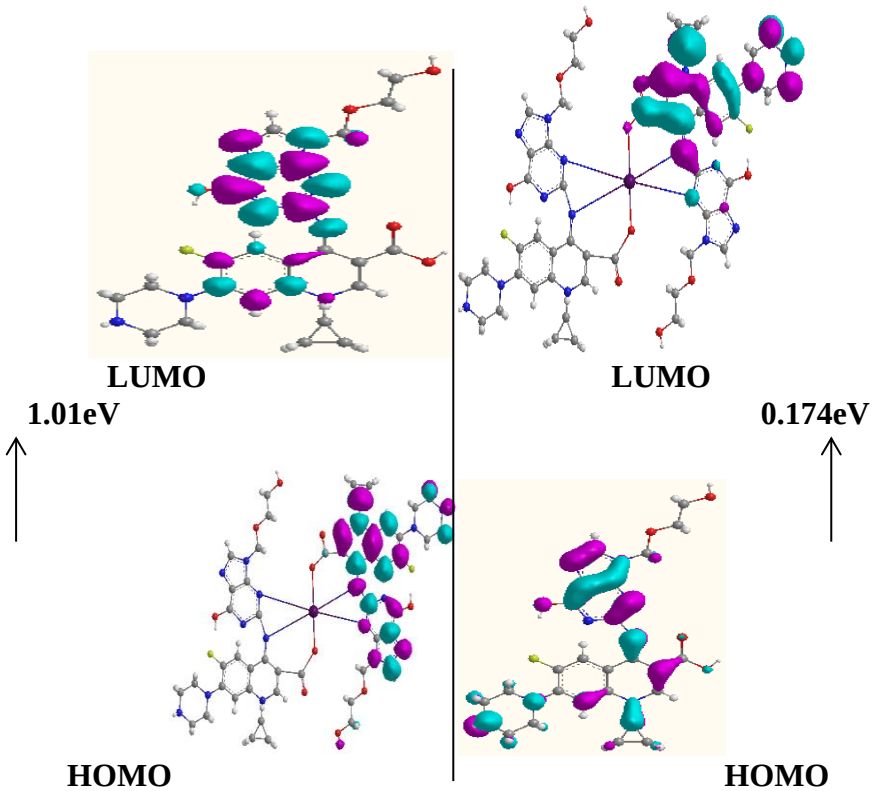

Figure 16: Complexes CCP frontier molecular orbitals; (a) Zn (II) complex (b) DFT calculations using B3LYP/LanL2DZ, level of theory color codes: Zn, red; N, blue; O, oxygen; and C, silver.

Table 6: Evaluated quantum chemical parameters of the CCP ligand and its compounds

Compound	LUMO (ev)	HOMO (ev)	ΔE	(χ)	μ	H	Σ	S	Ω
L = CCP	-3.516	-3.342	0.174	-3.429	3.429	0.088	11.492	5.747	**67.574**
Mn $(CCP)_2$	-4.093	-3.558	0.535	-3.825	3.8255	0.267	3.738	1.869	**22.735**
[Fe $(CCP)_2$]Cl	-3.572	-2.903	0.769	-3.187	0.318	0.384	2.600	1.300	**13.212**
Cu $(CCP)_2$	-4.831	-4.424	0.407	-4.627	4.6275	0.203	4.914	2.457	**52.613**
Zn $(CCP)_2$	-3.573	4.583	1.01	-4.078	4.078	0.505	1.980	0.990	**16.456**
Ca $(CCP)_2$	-4.633	-3.914	0.719	-4.273	4.2735	0.359	2.781	1.390	**25.400**

4. The biological activity

There have been a few breakthroughs for treating infectious diseases. Until 1915, they were all derived from natural sources. Ehrlich Paul found several helpful medications that were additional to the discipline of drugging known as chemotherapy, which involves the use of chemicals to treat bacterial illnesses. The substance that kills bacteria without harming the receptor tissue [39,40]. This investigation used two-bacterial genera; the influence of the ligand and equipped compounds in opposition to two species of bacteria was premeditated; nevertheless, in this experiment, the solvent was DMSO, the ligand was effective, direct bacteria were the medium of choice, and most complexes were in the medium-to-high range. Only fat-soluble chemicals are allowed in the surrounding cell, making fat solubility a crucial element in controlling the antibacterial action. As a result, the compound travels more quickly across the cell membrane and the lipid layers of the microbe barrier before entering and killing the bacterial cell [41,42]. Transitional elements, on the other hand, have antimicrobial properties [43].

Table 7 : Zone of inhibition of the ligand CCP and all compounds (mm)

Compound	*Escherichia coli*	*Pseudomonas Aeruginosa*	*Staphylococcus Aureus*	*Klebsiella pneumonia*
L= CCP	34	30	33	38
Mn $(CCP)_2$	18	24	22	21
[Fe $(CCP)_2$] Cl	41	38	43	42
Cu $(CCP)_2$	38	33	39	37
Zn $(CCP)_2$	29	29	37	29
Ca $(CCP)_2$	37	36	30	37
Control-DMSO	0	0	0	0
Ciprofloxacin	24	22	26	22
Acyclovir	28	24	28	25

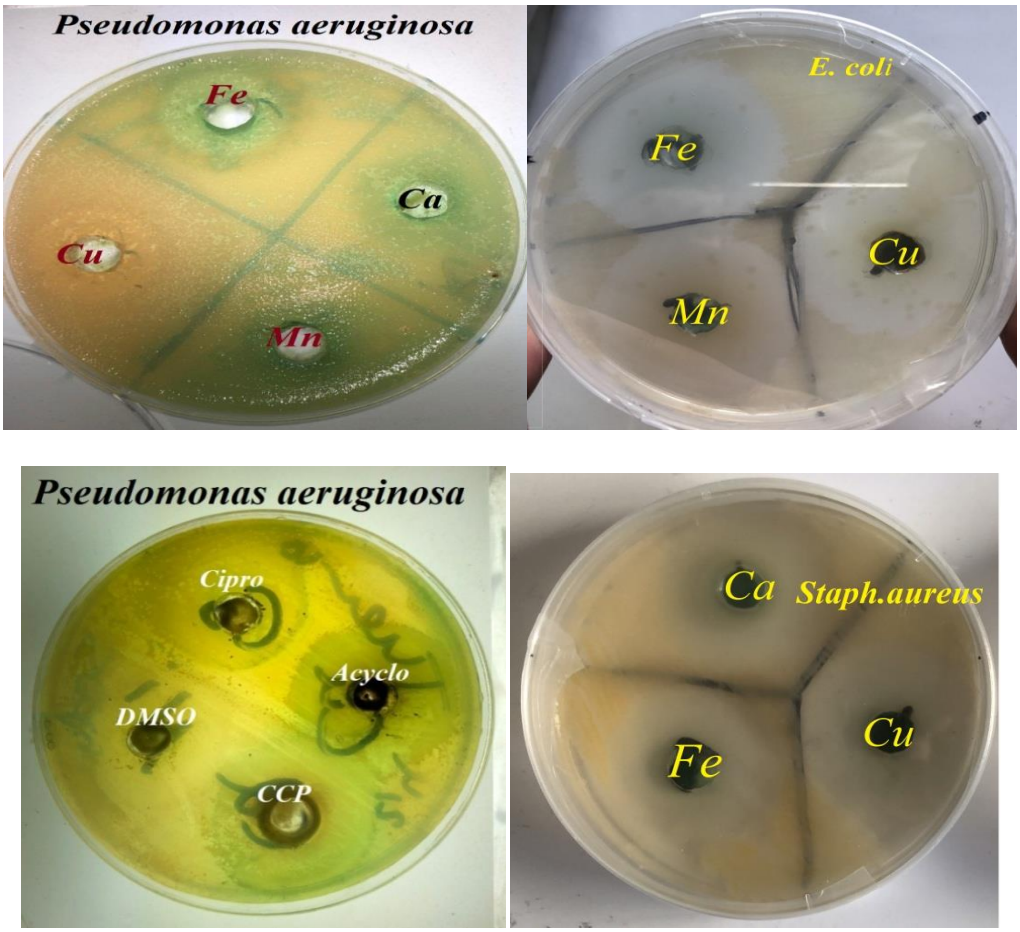

Figure 17: Zone of inhibition of bacterial growth (mm) bacteria image of CCP ligand and its complexes

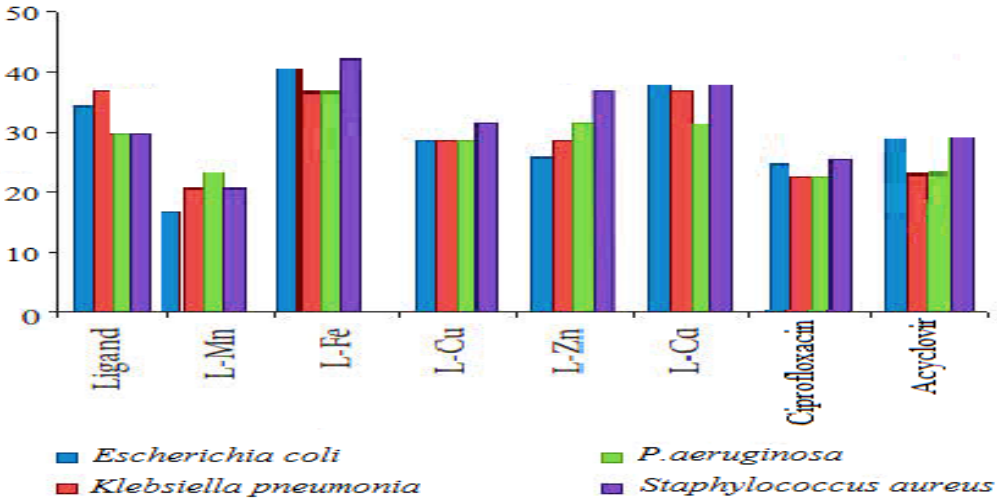

Figure 18: Biological activity of the CCP ligand and its complexes

5. Conclusion

A new Schiff base ligand, cyclopropyl-6-fluoro-4-(6-hydroxy-9-(2-hydroxyethoxy) methyl)-9H-purin-2-yl) imino)-7-(piperazin-1-yl)-1,4-dihydroquinoline-3-carboxylic acid), was synthesized and indulged by many brackish metals to provide the corresponding compounds. The original CCP ligand responded with the metal ions since 1M:2L the analytical statistics demonstrated that feedbacks of the gratis CCP ligand with Mn (II), Fe (III), Cu (II), Zn (II), and Ca (II) shaped complexes with chemical modus operandi ($[M(CCP)_2]$, M=Mn (II),

Cu (II), Zn (II), and Ca (II) and $[M(CCP)_2]$ Cl, (M = Fe (III)). The probable constructions of the ligand and complexes were wished-for pedestals resting on fundamental psychoanalysis, ^{1}H NMR, ^{13}C NMR, FT-IR, and UV-Vis electronic incorporation. Following the coordination to the metal ions, the CCP ligand behaved as a tridentate ligand with two atoms of N harmonization location and protonated carboxylate oxygen, resulting in the structure of octahedral geometries for each complex. In addition, molecular docking studies of the free ligand and the Zn (II) complex with the herpes simplex microbe kind-1 thymidine kinase and DFT calculation studies. *In vitro*, the ligands and complexes were divided in opposition to microbes (bacteria). The outcomes of natal bustle illustrated that the Fe (III) complex had stronger antiseptic effects against the (gram-positive) bacteria, even as Cu (II) had superior antibacterial motion not in favor of the (gram-negative) microorganisms compared to the free ligand and complexes. The biological effectiveness of the complexes was greater than that of the ligand.

References

[1] K. M. Hilmy, D. H. Soliman, E. B. Shahin, and R. Abd Al Hameed, "Synthesis and molecular modeling study of novel pyrrole Schiff Bases as anti-HSV-1 agents," Life *Science Journal*, vol. 9, no. 2, pp. 841-850, 2012.

[2] C. Y. Hsiang and T. Y. Ho, "Emodin is a novel alkaline nuclease inhibitor that suppresses herpes simplex virus type 1 yields in cell cultures," *British journal of pharmacology*, vol. 155, no. 2, pp. 227-235, 2008.

[3] J. T. Terry, B. J. Matthews, and A. K. Field, "The structure and function of the HSV DNA replication proteins: defining novel antiviral targets," *Antiviral research*, vol. 20, no. 2, pp. 89-114,1993.

[4] R. B. Tenser, "Role of herpes simplex virus thymidine kinase expression in viral pathogenesis and latency," *Intervirology*, vol. 32, no. 2, pp. 76-92, 1991.

[5] L. Aristilde and G. Sposito, "Molecular modeling of metal complexation by a fluoroquinolone antibiotic," *Environmental Toxicology and Chemistry: An International Journal*, vol. 27, no. 11, pp. 2304-2310, 2008.

[6] M. M. Ghorab, H. I. Heiba, A. I. Khalil, D. A. Abou El Ella and E. Noaman, "Computer-based ligand design and synthesis of some new sulfonamides bearing pyrrole or pyrrolopyrimidine moieties having potential antitumor and radioprotective activities," *Phosphorus, Sulfur, and Silicon and the Related Elements*, vol. 183, no. 1, pp. 90-104, 2007.

[7] M. P. Clark, K. M. George, R. G. Bookl and, J. Chen, S. K. Laughlin, K. D. Thakur and G. Zhang, "Development of new pyrrolopyrimidine-based inhibitors of Janus kinase 3 (JAK3)," *Bioorganic and medicinal chemistry letters*, vol. 17, no. 5, pp. 1250-1253, 2007.

[8] S. Merighi, P. Mirandola, K. Varani, S. Gessi, E. Leung, P. G. Baraldi and P. A. Borea, "A glance at adenosine receptors: novel target for antitumor therapy," *Pharmacology and therapeutics*, vol. 100, no. 1, pp. 31-48, 2003.

[9] K. J. Moriarty, H. K. Koblish, T. Garrabrant, J. Maisuria, E. Khalil, F. Ali, and R. A. GalemmoJr, "The synthesis and SAR of 2-amino-pyrrolo [2, 3-d] pyrimidines: a new class of Aurora-A kinase inhibitors," *Bioorganic and medicinal chemistry letters*, vol. 16, no. 22, pp. 5778-5783, 2006.

[10] D. A. Abou El Ella, M. M. Ghorab, E. Noaman, H. I. Heiba, and A. I. Khalil, "Molecular modeling study and synthesis of novel pyrrolo [2,3-d] pyrimidines and pyrrolotriazolopyrimidines of expected antitumor and radioprotective activities," *Bioorganic and medicinal chemistry*, vol. 16, no. 5, pp. 2391-2402, 2008.

[11] S. M. Hassan, A. A. El-Maghraby, M. M. Abdel Aal, and M. S. Bashandy, "Heteroaromatization with sulfonamido phenyl ethanone, part I: synthesis of novel pyrrolo [2, 3-d] pyrimidine and pyrrolo [3,2-E] [1,2,4] Triazolo [1,5-C] pyrimidine derivatives containing dimethyl sulfonamide moiety," *Phosphorus, Sulfur, and Silicon*, vol. 184, no. 2, pp. 291-308, 2009.

[12] E. M. Golet, A. C. Alder, and W. Giger, "Environmental exposure and risk assessment of fluoroquinolone antibacterial agents in wastewater and river water of the Glatt Valley Watershed, Switzerland," *Environmental science and technology*, vol. 36, no. 17, pp. 3645-3651, 2002.

[13] M. Imran, J. Iqbal, S. Iqbal, and N. Ijaz, "In vitro antibacterial studies of ciprofloxacin-imines and their complexes with Cu (II), Ni (II), Co (II), and Zn (II), "Turkish *journal of biology*, vol. 31, no. 2, pp. 67-72, 2007.

[14] A. O. Adekunle, I. T. Uzoigwe, P. N. Ndahi, and A. W. Omar, "Synthesis, Characterization and Antimicrobial Studies of Ni (II), Cu (II) and Mn (II) Complexes with Schiff Base derived from Ciprofloxacin and 2-Amino Pyridine," *Chemistry Research Journal*, vol. 4, no. 2, pp. 87-92, 2019.

[15] R. J. Hamilton, N. A. Duffy, and D. Eds. Stone, "Tarascon pharmacopoeia" Jones and Bartlett Publishers, 2014.

[16] J. N. Champness, M. S. Bennett, F. Wien, R. Visse, W. C. Summers, P. Herdewijn, and M. R. Sanderson, "Exploring the active site of herpes simplex virus type-1 thymidine kinase by X-ray crystallography of complexes with acyclovir and other ligands," *Proteins: Structure, Function, and Bioinformatics*, vol. 32, no. 3, pp. 350-361, 1998.

[17] A. Gueye, F. B. Tamboura J. M. Planeix, N. Gruber, and M. Gaye, "Synthesis and spectroscopic study of transition metal complexes of tridentate ligand formed by direct condensation of o-vanillin and 2-aminophenol: X-ray structural characterization of the zinc (II) complex, "European *Journal of Chemistry*, vol. 9, no. 4, pp. 281-286, 2018.

[18] V. P. Raju, R. Vedantham, M. D. Khunt, V. T. Mathad, P. K. Dubey, and A. K. Chakravarthy, "An Efficient and Large-Scale Process for Synthesis of Val acyclovir," Asian *Journal of Chemistry*, vol. 22, no. 5, pp. 4092, 2010.

[19] M. Zupančič, I. Turel, P. Bukovec, A. J. White, and D. J. Williams, "Synthesis and Characterization of Two Novel Zinc (II) Complexes with Ciprofloxacin Crystal Structure of $[C_{17}H_{19}N_3O_3F]_2 \cdot [ZnCl_4]. 2H_2O$," Croatica *ChemicaActa*, vol. 74, no.1, pp. 61-74, 2001.

[20] P. Drevenšek, J. Košmrlj, G. Giester, T. Skauge, E. Sletten, K. Sepčić, and I. Turel, "X-Ray crystallographic, NMR and antimicrobial activity studies of magnesium complexes of fluoroquinolones-racemic ofloxacin and its S-form, levofloxacin," *Journal of inorganic biochemistry*, vol. 100, no. 11, pp. 1755-1763, 2006.

[21] S. A. Sadeq, M. S. El-Attar, and S. M. Abd El-Hamid, "Synthesis and characterization and antibacterial activity of some new transition metal complexes with ciprofloxacin-imine," Bulletin *of the Chemical Society of Ethiopia*, vol. 29, no. 2, pp. 259-274, 2015.

[22] R. Kothari, B. Sharma, Sahiwal, K. Neha, S. Mandal, S. Birthare, and V. Shikhara, "Synthesis, characterization and antimicrobial evaluation of copper (II) complex with ciprofloxacin antibiotic," *World Journal of Pharmacy and Pharmaceutical Sciences*, vol. 4, no. 6, pp. 696-707, 2015.

[23] A. H. Noor Al-Huda Al-Mohammadi, A. S. M. Al-Fahdawi, and S. S. I. AL-Janabi, "Design and Characterization of New Di nuclear Macrocyclic Di thiocarbamate Complexes by the Preparation of a Free Ligand Derived from Isopropyl amine," *Iraqi Journal of Science*, vol. 62, no.1, pp.1-15, 2021.

[24] N. Raman, S. Esther, and C. Thangaraja, "A new Manniche base and its transition metal (II) complexes-synthesis, structural characterization and electrochemical study," *Journal of Chemical Sciences*, vol. 116, no. 4, pp. 209-213, 2004.

[25] E. I. Obasuyi and O. Iyekowa, "Synthesis, Characterization and Antimicrobial of Schiff Base from 5-Bromo-Salicylaldehyde and P-Toluidine,". *Journal of Applied Sciences and Environmental Management*, vol. 22, no. 11, pp. 1733-1736, 2018.

[26] R. Kothari, B. Sharma, S. Sahiwal, K. Neha, S. Mandal, S. Birthare, and V. Shikhara, "Synthesis, characterization and antimicrobial evaluation of copper (II) complex with ciprofloxacin antibiotic," *World Journal of Pharmacy and Pharmaceutical Sciences*, vol. 4, no. 6, pp. 696-707, 2015.

[27] H. Xu, K. C. Zheng, H. Deng, L. J. Lin, Q. L. Zhang, and L. N. Ji, "Effects of the ancillary ligands of polypyridyl ruthenium (II) complexes on the DNA-binding behaviors," *New Journal of Chemistry*, vol. 27, no. 8, pp. 1255-1263, 2003.

[28] P. Sengupta, R. Dida, and S. Ghosh, "Ruthenium (II) complexes of NSO donor ligands in the form of ring-substituted 4-phenyl-thiosemicarbazones of salicylaldehyde and o-hydroxy acetophenone," Transition *metal chemistry*, vol. 27, no. 6, pp. 665-667, 2002.

[29] J. N. Champness, M. S. Bennett, F. Wien, R. Visse, W. C. Summers, P. Herdewijn, and M. R. Sanderson, "Exploring the active site of herpes simplex virus type-1 thymidine kinase by X-ray

crystallography of complexes with acyclovir and other ligands," *Proteins: Structure, Function, and Bioinformatics*, vol. 32, no. 3, pp. 350-361, 1998.

[30] C. Scholz, S. Knorr, K. Hama Cher, and B. Schmidt, "Docktiteff A Highly Versatile Step-by-Step Workflow for Covalent Docking and Virtual Screening in the Molecular Operating Environment," *Journal of chemical information and modeling*, vol. 55, no. 2, pp. 398-406, 2015.

[31] S. Li, Y. Zhou, W. Lu, Y. Zhong, W. Song, K. Liu, and H. Li, "Identification of inhibitors against p90 ribosomal S6 kinase 2 (RSK2) through structure-based virtual screening with the inhibitor-constrained refined homology model," Journal *of chemical information and modeling*, vol. 51, no. 11, pp. 2939-2947, 2011.

[32] R. I. H. Al-Bayit, F. R. Mahdi, and A. A. H. Al-Amery, "Synthesis, spectroscopic and antimicrobial studies of transition metal complexes of N-amino quinolone derivatives," British *Journal of Pharmacology and Toxicology*, vol. 2, no. 1, pp. 5-11, 2011.

[33] A. N. MA Alaghaz and S. A. Aldulmani, "Preparation, Structural characterization and DNA binding/cleavage affinity of new bioactive nano-sized metal (II/IV) complexes with ox Azon-Schiff's base Ligand," *Applied Organometallic Chemistry*, vol. 33, no. 10, p. e5135, 2019.

[34] Z. Yekke-ghasemi, R. Takjoo, M. Ramazani, and J. T. Maguey, "Molecular design and synthesis of new dithiocarbazate complexes; crystal structure, bioactivities and nano studies," *RSC advances*, vol. 8, no. 73, pp. 41795-41809, 2018.

[35] Z. Parsee and K. Mohammadi, "Synthesis, characterization, nano-sized binuclear nickel complexes, DFT calculations and antibacterial evaluation of new macrocyclic Schiff base compounds," *Journal of Molecular Structure*, vol. 1137, no. 5, pp. 512-523, 2017.

[36] F. Sama, M. Raizada, M. Ashfaq, M. N. Ahamad, I. Mantashe, K. Iman, and H. A. Saleh, "Synthesis, structure and DNA binding properties of a homonuclear Cu (II) complex: An experimental and theoretical approach," *Journal of Molecular Structure*, vol. 1176, no. 15, pp. 283-289, 2019.

[37] O. A. El-Gemmal, A. F. Al-Hosseini, and S. A. El-Brashly, "Spectroscopic, DFT, optical band gap, powder X-ray diffraction and bleomycin-defendant DNA studies of Co (II), Ni (II) and Cu (II) complexes derived from macrocyclic Schiff base," *Journal of Molecular Structure*, vol. 1165, no.5, pp. 177-195, 2018.

[38] M. Govindarajan, S. Periandy, and K. Carthigayen, "FT-IR and FT-Raman spectra, thermo dynamical behavior, HOMO and LUMO, UV, NLO properties, computed frequency estimation analysis and electronic structure calculations on α-bromo toluene," *Spectrochemical Acta Part A: Molecular and Biomolecular Spectroscopy*, vol. 97, no. 11, pp. 411-422, 2012.

[39] L. Ravishankar, S. A. Pat we, N. Go Sarani, and A. Roy, "Cerium (III)-catalyzed synthesis of Schiff bases: a green approach," *Synthetic Communications*, vol. 40, no. 21, pp. 3177-3180, 2010.

[40] Z. G. Alrecabi, R. A. J. Al-Fraiji, and S. M. H. Al-Majidi, "Synthesis, Identification of Some New Derivatives of Oxazepane, Thiazinone and Hydro quinazoline and Evaluation of Antibacterial Activity," *Iraqi Journal of Science*, vol. 58, no. 3c, pp. 1565-1566, 2017.

[41] A. H. Caswell and B. C. Pressman, "Kinetics of transport of divalent cations across sarcoplasmic reticulum vesicles induced by ionophores," *Biochemical and biophysical research communications*, vol. 49, no. 1, pp. 292-298, 197

[42] J. Hernández-Borrell and M. T. Montero, " Calculation micro species concentration of zwitterion amphoteric compounds: ciprofloxacin as example," *Journal of chemical education*, vol. 74, no. 11, p. 1311, 1997.

[43] M. Palumbo, B., Gatto, G. Zagato, and G. Palù, "On the mechanism of action of quinolone" *Trends in microbiology*, vol. 1, no. 6, pp. 232-235, 1993.